ChemComm

COMMUNICATION

View Article Online
View Journal | View Issue

Unveiling the electronic origin of anion order in $CrO_{2-x}F_x$†

Cite this: *Chem. Commun.*, 2014, 50, 799

Received 18th August 2013,
Accepted 23rd October 2013

DOI: 10.1039/c3cc46336b

www.rsc.org/chemcomm

Bing Li,*[ab] Yanna Chen,[ab] Hui Wang,[ab] Wen Liang,[c] Guangyao Liu,[c] Weijun Ren,[ab] Caifu Li,[a] Zhiquan Liu,[a] Guanghui Rao,[cd] Changqing Jin[c] and Zhidong Zhang*[ab]

Electron-diffraction and high-resolution lattice images reveal superstructure stripes with wave vectors of (1/3, 0, 1/3) and (−1/3, 0, 1/3), which are associated with the ordered arrangement of F^-. Charge density distribution suggests that these stripes manifest themselves electronically as F^-–Cr^{3+}–F^- zigzag chains, driven by the anisotropic charge interaction of F^- anions.

Correlated anion order in transition-metal mixed-anion systems is a fundamental issue of solid state chemistry and its close connection with novel functionalities has been demonstrated in a great diversity of systems.[1] As one of the most common representatives, anion order between F^- and O^{2-} has been investigated in a rich variety of oxyfluorides.[2] The interest in such an order was initially stimulated by the founding of high-T_c superconductivity in fluorinated cuprates. In $Nd_2CuO_{4-x}F_x$ and $Sr_2CuO_2F_{2+\delta}$, F^- anions show a site-preference for the apical sites with the CuO_2 plane intact.[3,4] F^-/O^{2-} anion order has recently been found in other transition-metal (Fe, Co, Mo, and W) compounds.[5–11] However, the exact origin of F^-/O^{2-} ordering has not been clarified so far, even though understanding this order in depth will potentially enable the design of novel materials. In this work, by a complementary study of experiments and electronic structure calculations, we have found anion ordering in oxyfluorides $CrO_{2-x}F_x$, with wave vectors of (1/3, 0, 1/3) and (−1/3, 0, 1/3), as the first observation in chromium oxyfluorides. Differential charge density distribution reveals strongly anisotropic charge interaction between anions and cations, which leads to zigzag chains consisting of F^-–Cr^{3+}–F^- in the long-range.

CrO_2 is a correlated ferromagnetic (FM) half-metal.[12] Goodenough proposed a model to understand the magnetism of CrO_2 from the viewpoint of molecular orbitals.[13] Korotin *et al.* explained the ferromagnetism of CrO_2 within the framework of double-exchange interaction by the LDA + U method.[12] $CrO_{2-x}F_x$ samples were first synthesized by Chamberland *et al.* and the rutile-type structure was identified at $x < 0.20$.[14] The magnetization was also measured down to low temperatures.

The nature of single phase $CrO_{2-x}F_x$ (x = 0.1, 0.12 and 0.14) samples was confirmed by X-ray diffraction (XRD) patterns, where only Bragg diffractions of rutile-type structures appeared, as shown in Fig. 1(b), for x = 0.14. The cell dimensions were evaluated and revealed that a is 0.44379(4) nm and c is 0.29221(5) nm for x = 0.1, 0.44390(1) nm and 0.29222(1) nm

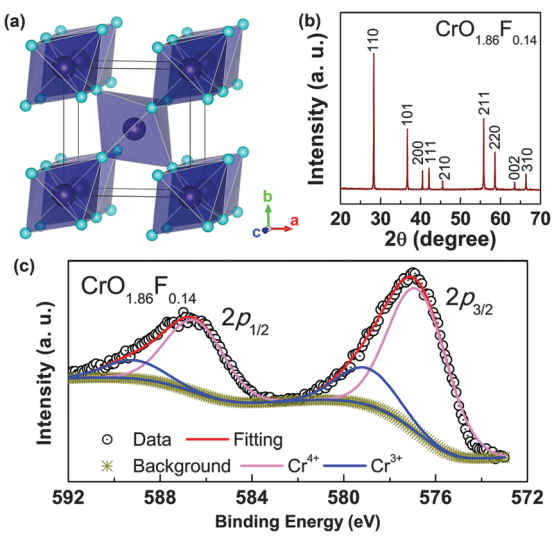

Fig. 1 (a) Crystal structure of $CrO_{2-x}F_x$, with the $Cr(O/F)_6$ octahedra highlighted. (b) XRD pattern of $CrO_{1.86}F_{0.14}$ at room temperature. (c) XPS profiles and fitting of $CrO_{1.86}F_{0.14}$.

[a] *Shenyang National Laboratory for Materials Science, Institute of Metal Research, Chinese Academy of Sciences, Shenyang 110016, China. E-mail: binglimag@gmail.com, zdzhang@imr.ac.cn; Fax: +86-24-23971205; Tel: +86-24-23971859*
[b] *International Center for Materials Physics, Chinese Academy of Sciences, Shenyang 110016, China*
[c] *Beijing National Laboratory for Condensed Matter Physics, and Institute of Physics, Chinese Academy of Sciences, Beijing 100190, China*
[d] *School for Materials Science and Technology, Guilin University of Electronic Technology, Guilin 541004, China*

† Electronic supplementary information (ESI) available. See DOI: 10.1039/c3cc46336b

for x = 0.12, and 0.44504(4) nm and 0.29267(6) nm for x = 0.14, respectively. This is consistent with previous reports in which the actual composition was determined to be almost identical to the nominal one.[14] Thus, the composition x presented here is considered as the actual composition. The crystal structure of $CrO_{2-x}F_x$ displayed in Fig. 1(a), is characterized by the octahedra of $Cr(O/F)_6$ surrounding the metal cations at the body centre and at corner sites, respectively, which differ by a 90° rotation about the c axis. The X-ray photoelectron spectroscopy (XPS) profiles of doped samples show peaks at 685.0 eV, which were assigned as F^- 1s and are indicative of F^- doping. In Fig. 1(c), XPS profiles from high-resolution scans around a binding energy window of metal cations show two broadened peaks, which are assigned to $2p_{1/2}$ and $2p_{3/2}$, respectively.[15,16] As with other mixed-valance systems, like $CuIr_2S_4$ and $Na_xV_2O_5$,[17,18] the collected profiles can be well fitted as a combination from two cations. Peaks of $2p_{1/2}$ and $2p_{3/2}$ for Cr^{4+} appear at 586.2 eV and 576.4 eV, while those for Cr^{3+} appear at 589.2 eV and 579.2 eV, respectively. The signals of Cr^{3+} for x = 0.1 and 0.12 come close to the background, while x = 0.14 clearly displays the contribution from Cr^{3+}.

DC magnetization measurements suggest that $CrO_{1.90}F_{0.10}$ and $CrO_{1.88}F_{0.12}$ are FM with a Curie temperature of about 300 K and 280 K, respectively. There is no obvious thermal hysteresis at the temperature dependencies of the field-cooled and field-warmed magnetization. Magnetism of $CrO_{1.86}F_{0.14}$ is much more complex due to the antiferromagnetic (AFM) to FM transition around 80 K, apart from the reduced Curie temperature.[19] Electronic structure calculations were employed to understand the magnetic behaviour.[20] A half-metal behaviour was found at FM coupling, with two kinds of Cr cations in spin charges, which were defined as Cr^{3+} and Cr^{4+}, respectively. These two kinds of cations both have xy localized states, and xz and yz itinerant states from the partial electronic density of states. Such special electronic states facilitate the double-exchange interaction, as shown in pure CrO_2.[12] When magnetic moments of magnetic cations locating at oxygen octahedra with different orientations (see Fig. 1(a)) are antiferromagnetically coupled, as considered in pure CrO_2,[12] an insulating behaviour is observed with a band gap of about 0.2 eV. The presence of an AFM insulator confirms the double-exchange mechanism. The mixed-valance feature is compatible with the magnetism in the framework of double-exchange interaction.

The microstructures of $CrO_{2-x}F_x$ were examined using a transmission electron microscope (TEM). The samples are easy to cleave into small pieces with a typical size of about 5 μm × 5 μm, as shown in Fig. 2(a). A [010] zone-axis electron-diffraction pattern of $CrO_{1.90}F_{0.10}$ at room temperature is displayed in Fig. 2(b). It is evident that there are superlattice spots with relatively weaker intensity in addition to the fundamental Bragg diffractions. The fundamental spots were indexed on the known rutile-type crystal structure with lattice parameters consistent with those from the XRD results. The sharp superlattice diffraction spots are assigned to the superstructures of (1/3, 0, 1/3) and (−1/3, 0, 1/3). The superlattice diffractions are also visible in the electron-diffraction pattern of the $[1\bar{3}\bar{1}]$ zone-axis, as shown in Fig. 2(c). These electron-diffraction patterns, belonging to two independent zone-axes, verify the occurrence of superstructures. We display the corresponding high-resolution lattice image of the superstructure of (−1/3, 0, 1/3) in Fig. 2(d), which undoubtedly indicates an extra periodicity. The actual electron-diffraction patterns are a mixture of these two superstructures (the incident electron beam for our diffraction experiments covers an area with a size of about 200 nm × 200 nm). The planar spacing of 0.25 nm corresponds to {101} crystallographic planes. The extra periodicity is obviously demonstrated in an intensity profile scanned along the direction perpendicular to the stripes (inset of Fig. 2(d)). We used an *in situ* heating TEM facility to track the evolution of superlattice spots and observed that they were still clear even at 573 K, as shown in the inset of Fig. 2(a). This suggests that the superstructures are stable at elevated temperatures, close to the decomposing temperature of pure CrO_2 at ambient conditions. Such superstructures have also been observed in $CrO_{1.88}F_{0.12}$ and $CrO_{1.86}F_{0.14}$.

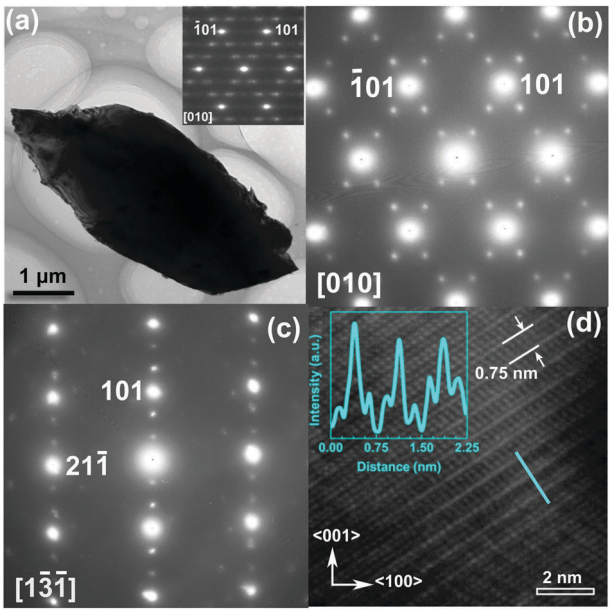

Fig. 2 (a) The typical morphology of $CrO_{1.90}F_{0.10}$. The inset shows the [010] zone-axis electron-diffraction pattern at 573 K. (b) A [010] zone-axis electron-diffraction pattern at room temperature. (c) A $[1\bar{3}\bar{1}]$ zone-axis electron-diffraction pattern. (d) The high-resolution lattice image related to the superstructure of (−1/3, 0, 1/3). The distance between two stripes is shown as 0.75 nm. The inset shows an intensity trace, along the direction perpendicular to the stripe, as indicated by the green line.

The first-principle electronic structure calculations were employed to reveal the distribution of charge. The initial structure model for the calculation was considered as a 3 × 3 × 3 supercell of the rutile-type structure ($Cr_{54}O_{102}F_6$) with pairing of F and Cr along the ⟨111⟩ direction, in which the Cr–F bond length and Cr–O bond length are equivalent. It is evident that there are two distinct profiles in the calculated differential charge density (Fig. 3(a)), with spin charges that are close to the pure ionic limits of Cr^{4+} and Cr^{3+}, respectively. Given the XPS results and magnetic double-exchange interaction mentioned above, it is reasonable to assign them as Cr^{4+} and Cr^{3+},

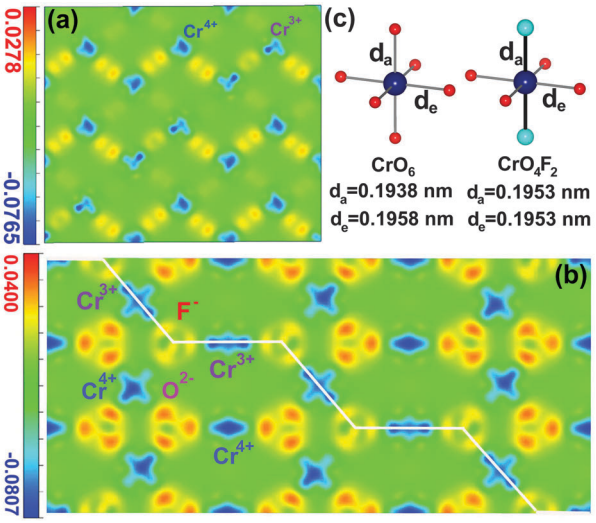

Fig. 3 (a) and (b) Differential charge density on the (101) and [1$\bar{1}$0] planes of $Cr_{54}O_{102}F_6$, respectively. The differential charge density is in units of eV Å^{-3}. The zigzag line indicates the F^-–Cr^{3+}–F^- ion chains. (c) The apical (d_a) and equatorial (d_e) bond length for CrO_6 (left) and CrO_4F_2 (right) octahedral configurations in this optimized structure.

as labelled in Fig. 3(a). It is through F^- doping that Cr^{3+} cations are created between the two nearest closed F^- anions along the ⟨111⟩ direction, which brings out exotic ionic zigzag chains consisting of F^-–Cr^{3+}–F^-, as shown in Fig. 3(b). The electronic effect of F^- anions on the system is strongly anisotropic. F^- anions mainly attract electrons from the cations on the zigzag chains. By contrast, the effect of O^{2-} anions is nearly isotropic. Thus, the occurrence of anion ordering is attributed to such anisotropic charge interaction.

Local structural distortion associated with F^- doping is discerned in the optimized structure of the first-principle electronic structure calculation. In Fig. 3(c), we plot the CrO_6 and CrO_4F_2 octahedral configurations in this optimized structure. A compressed octahedral atmosphere ($d_e - d_a = 0.02$ nm), similar to that in pure CrO_2, is found for CrO_6, whereas CrO_4F_2 shows a nearly isotropic configuration. The experimentally observed electron-diffraction patterns can be reproduced based on this model, which suggests that the superstructure model is highly possible.

It is well-known that CrO_2 is a metastable oxidation state of Cr in ambient conditions and the stable form is Cr_2O_3.[21] As a consequence, CrO_2 heated in air tends to lose oxygen atoms and produces vacancies, which may exhibit long-range order, such as in cuprate superconductors.[22] In TEM studies on the reduced CrO_2, we did not observe any superstructure diffraction. Consequently, the superstructures observed in $CrO_{2-x}F_x$ are attributed to an ordered arrangement of F^-.

To summarize, the oxyfluorides $CrO_{2-x}F_x$ of a single phase were synthesized at a high-pressure. High-resolution XPS suggests the mixed-valance feature of Cr^{4+} and Cr^{3+} in this compound, consistent with magnetic double-exchange interaction. The stripes associated with the ordered arrangement of F^- are observed with wave vectors of (1/3, 0, 1/3) and (−1/3, 0, 1/3) in electron-diffraction patterns and high-resolution lattice images, originating from local structure distortion induced by F^- doping. Electronic structure calculations reveal the strongly anisotropic charge interaction of F^- anions, which results in anion ordering and ion-pairing F^-–Cr^{3+}–F^- zigzag chains. Therefore, the anion ordering and ion-pairing stripes are regarded as being electronic in nature.

We would like to thank Dr Qingqing Liu for assistance with the high-pressure synthesis and Wenjie Gong for helping with the transmission electron microscopy characterizations. We also thank Prof. Xingqiu Chen for the valuable discussions on electronic structure calculation. This work has been supported by the National Natural Science Foundation of China under Grant No. 50831006.

Notes and references

1 Y. Tsujimoto, K. Yamaura and E. Takayama-Muromachi, *Appl. Sci.*, 2012, **2**, 206.
2 C. Greaves and M. G. Francesconi, *Curr. Opin. Solid State Mater. Sci.*, 1998, **3**, 132.
3 A. C. W. P. James, S. M. Zahurak and D. W. Murphy, *Nature*, 1989, **338**, 240.
4 M. Al-Mamouri, P. P. Edwards, C. Greaves and M. Slaski, *Nature*, 1994, **368**, 382.
5 R. L. Needs, M. T. Weller, U. Scheler and R. K. Harris, *J. Mater. Chem.*, 1996, **6**, 1219.
6 L. D. Aikens, R. K. Li and C. Greaves, *Chem. Commun.*, 2000, 2129.
7 A. L. Hector, J. A. Hutchings, R. L. Needs, M. F. Thomas and M. T. Weller, *J. Mater. Chem.*, 2001, **11**, 527.
8 F. J. Berry, F. C. Coomer, C. Hancock, Ö. Helgason, E. A. Moore, P. R. Slater, A. J. Wright and M. F. Thomas, *J. Solid State Chem.*, 2011, **184**, 1361.
9 Y. Tsujimoto, K. Yamaura, N. Hayashi, K. Kodama, N. Igawa, Y. Matsushita, Y. Katsuya, Y. Shirako, M. Akaogi and E. Takayama-Muromachi, *Chem. Mater.*, 2011, **23**, 3652.
10 Y. Tsujimoto, J. J. Li, K. Yamaura, Y. Matsushita, Y. Katsuya, M. Tanaka, Y. Shirako, M. Akaogi and E. Takayama-Muromachi, *Chem. Commun.*, 2011, **47**, 3263.
11 A. M. Fry, H. A. Seibel, I. N. Lokuhewa and P. M. Woodward, *J. Am. Chem. Soc.*, 2012, **134**, 2621.
12 M. A. Korotin, V. I. Anisimov, D. I. Khomskii and G. A. Sawatzky, *Phys. Rev. Lett.*, 1998, **80**, 4305.
13 J. B. Goodenough, *Metallic Oxides in Solid State Chemistry*, ed. H. Reiss, Pergamon, 1971.
14 B. I. Chamberland, C. G. Frederick and J. L. Gillson, *J. Solid State Chem.*, 1973, **6**, 561.
15 I. Ikemoto, K. Ishii, S. Kinoshita, H. Kuroda, M. A. Alario Franco and J. M. Thomas, *J. Solid State Chem.*, 1976, **17**, 425.
16 D. Shuttleworth, *J. Phys. Chem.*, 1980, **84**, 1629.
17 K. Takubo, S. Hirata, J.-Y. Son, J. W. Quilty, T. Mizokawa, N. Matsumoto and S. Nagata, *Phys. Rev. Lett.*, 2005, **95**, 246401.
18 M. J. Konstantinović, S. Van den Berghe, M. Isobe and Y. Ueda, *Phys. Rev. B*, 2005, **72**, 125124.
19 B. Li, W. Liang, W. J. Ren, W. J. Hu, J. Li, C. Q. Jin and Z. D. Zhang, *Appl. Phys. Lett.*, 2012, **100**, 242408.
20 G. Kresse and J. Hafner, *Phys. Rev. B*, 1993, **47**, 558.
21 H. Y. Hwang and S. W. Cheong, *Science*, 1997, **278**, 1607.
22 J. M. Sanchez, F. Mejialira and J. L. Moranlopez, *Phys. Rev. B*, 1988, **37**, 3678.